R. & M. No. 3201

R. & M. No. 3201
(21,404)
A.R.C. Technical Report

MINISTRY OF AVIATION

AERONAUTICAL RESEARCH COUNCIL
REPORTS AND MEMORANDA

Approximate Calculation of Three-Dimensional Laminar Boundary Layers

By J. C. Cooke, M.A.

LONDON: HER MAJESTY'S STATIONERY OFFICE
1961
PRICE 12s. 0d. NET

Approximate Calculation of Three-Dimensional Laminar Boundary Layers

By J. C. Cooke, M.A.

Communicated by the Deputy Controller Aircraft (Research and Development)
Ministry of Supply

Reports and Memoranda No. 3201*

October, 1959

Summary.—Three different approximate methods of solving the three-dimensional laminar boundary-layer equations are tested on a problem whose exact solution is known. From the comparison one of the methods, which is developed in this paper, is recommended as the one to use in general, provided that the cross-flow in the boundary layer is not large.

The method is tested on two allied problems whose exact solution is known; fair agreement is obtained.

Finally the three methods are used to find the angle between streamlines and limiting streamlines for the flow over a slender delta wing, and to determine the point of separation.

1. *Introduction.*—Very few exact solutions of the three-dimensional laminar boundary-layer equations exist, even in the incompressible case. Those that do are rather special cases, such as the infinite sheared wing, for which by the 'independence principle' the flow normal to the generators can be determined from a two-dimensional solution, leaving the cross-flow velocity still to be determined. Even in this case an exact solution only exists as a series whose convergence is usually such that the solution does not extend very far downstream. A finite exact solution of a family of three-dimensional boundary-layer problems has been given by Hansen and Herzig[1]. This family is not very realistic in that (as in the infinite sheared wing problem) the external streamlines are translates. Its great advantage is that the solution is given as a finite series and may be continued as far downstream as may be desired. The external flow is not irrotational, but this does not preclude this solution being used as a test. The external flow is such that the velocity components over the surface $\zeta = 0$, which is a plane, are of the form

$$\left.\begin{aligned} U_1 &= \text{const} \\ V_1 &= \sum_{r=0}^{N'} a_r x^r \end{aligned}\right\} \qquad (1)$$

in the x and y directions respectively, the suffix $_1$ referring to main-stream conditions. Hansen and Herzig have worked out the solution for any positive integral value of N' up to 10.

* R.A.E. Tech. Note Aero. 2658, received 16th November, 1959.

We shall test the method of Eichelbrenner and Oudart[2], the method of Zaat[3] and a method which is a modification of that of Zaat; our conclusions lead us to recommend the latter for general use.

All these methods use streamline co-ordinates and assume that the velocity in the boundary layer normal to the external streamlines is small. (In speaking generally of this velocity we shall use the term 'cross-flow' to distinguish it from the streamwise flow). Since the cross-flow velocity is zero on the surface of the body and zero at the edge of the boundary layer the assumption of small cross-flow seems a reasonable one to make. The equations governing the flow in the streamwise direction can then be reduced, by a Mangler transformation, into ordinary two-dimensional boundary-layer equations which may be solved in ways well known.

All the methods considered here are based on the momentum equations. They differ in the choice of velocity profiles. For the streamwise flow all use a one parameter family. Eichelbrenner and Oudart[2] choose a Pohlhausen quartic, whilst in Zaat's[3] and the present method profiles of the Timman[4] type are used. The methods differ widely in their manner of treating the cross-flow. Here Eichelbrenner and Oudart[2] use a Pohlhausen cubic, with the same boundary-layer 'thickness' as before, together with a multiplying parameter whose value is obtained by satisfying a boundary condition on the surface of the body. Consequently this parameter is determined without solving the cross-flow equation which is not in fact satisfied. The other two methods require the solution of the cross-flow equation and this allows the inclusion of an additional parameter in the representation of the cross-flow profiles. The main difference betweem them lies in the choice of this additional parameter.

Thus Zaat[3] uses similar profiles (originally due to Timman[5]) with an extra parameter Ω relating the 'thicknesses' of the boundary layer in the two directions. The assumption of similarity is very far from the truth near a point of inflexion in the external streamlines, as can be seen in Fig. 1. This Figure has been drawn from calculations based on an exact solution by Hansen and Herzig[1] and shows how different in shape the cross-flow velocity profiles can be at different points along an external streamline. The assumption of similarity also leads to the result that the cross-flow velocity is zero at all points immediately underneath an external point of inflexion, and changes its direction (*i.e.*, its sign) simultaneously at all such points as the external streamlines change from concave to convex or *vice versa*. Fig. 1 shows that the cross-flow velocity near a point of inflexion may have different signs at different parts of the boundary layer, thus violating the assumption.

To correct this, Zaat[11, 12] later modified his cross-flow profiles by the introduction of a second parameter K and a second profile, to carry the solution past the point of inflexion and thus avoid the undesirable features of the earlier method (*See* Appendix I for details).

In the present recommended method the undesirable features in the cross-flow profile are avoided another way. In fact we go back to Timman's original scheme[6] in which an additional parameter Π is inserted into the cross-flow velocity, and the previous parameter Ω, related to the ratio of the boundary layer 'thicknesses', is dropped.

It may be noted that after making the assumption of small cross-flow and applying the Mangler transformation[7] the method of Thwaites[8] may be used for the streamwise flow. We have included this also in our test, as far as the streamwise flow is concerned.

We have compared the various methods in our first example and find that the present recommended method is the best for the example shown. It is outlined in Section 2. We have also compared the solution by the recommended method with the exact solution for two further allied examples and have found good agreement. Finally the present method, Zaat's first method, and that of Eichelbrenner and

Oudart have been used to calculate the boundary-layer development on a delta wing of 72-deg sweep. The correct solution is not known in this case, but it is of interest, nevertheless, to make such a comparison, which is carried through as far as separation.

2. *The Recommended Approximate Method.*—We take a streamline co-ordinate system on the surface where the line element ds is given by

$$ds^2 = \frac{1}{U^2\rho_1}\,d\phi^2 + \frac{1}{U^2\rho_2}\,d\psi^2, \tag{2}$$

where the curves $\psi = \text{const.}$ are streamlines and the curves $\phi = \text{const.}$ are their orthogonal trajectories. If a velocity potential exists we may denote it by ϕ and take $\rho_1 = 1$, $\rho_2 = \bar{\rho}$ as is done by Timman and Zaat. U is here the resultant external velocity.

The determination of $\bar{\rho}$ is described by Zaat[3] and by Cooke[9]. We give here only the form taken by $\bar{\rho}$ when the surface $\zeta = \zeta(x,y)$ is sufficiently flat for partial derivatives of ζ with respect to x and y to be small.

We then have

$$\frac{1}{\bar{\rho}}\frac{\partial\bar{\rho}}{\partial\phi} = -\frac{2}{U^2}\left(\frac{\partial U_1}{\partial x} + \frac{\partial V_1}{\partial y}\right),$$

$$U^2\frac{\partial}{\partial\phi} = U_1\frac{\partial}{\partial x} + V_1\frac{\partial}{\partial y},$$

$$U^2\sqrt{\bar{\rho}}\,\frac{\partial}{\partial\psi} = V_1\frac{\partial}{\partial x} - U_1\frac{\partial}{\partial y}.$$

In the method we use the velocity profiles

$$\frac{u}{U} = f(z) - \Lambda g(z),$$

$$\frac{v}{U} = \Pi h(z) - Mg(z),$$

where

$$\zeta = \sqrt{(\sigma\nu)}z, \quad 1 - f(z) = 2g(z) + e^{-z^2} = \frac{2}{3\sqrt{\pi}}\,z\,e^{-z^2} + \frac{2}{\sqrt{\pi}}\int_z^\infty e^{-t^2}\,dt,$$

$$h(z) = z\,e^{-z^2},$$

$$\Lambda = \sigma U\frac{\partial U}{\partial\phi}, \qquad M = \sqrt{\bar{\rho}}\,\sigma U\frac{\partial U}{\partial\psi}. \tag{3}$$

σ is a parameter determined in the solution. It is related to the streamwise momentum thickness Θ_{11} by the equation

$$\Theta_{11} = 0{\cdot}293\,\sqrt{(\sigma\nu)}, \tag{4}$$

which is approximately true for the profiles given above.

We find, as shown in Appendix II, that the equations to be solved are

$$\frac{\partial}{\partial\bar{\phi}}\left(\frac{U^4\sigma}{\bar{\rho}}\right) = 5{\cdot}08\,\frac{U^2}{\bar{\rho}}, \tag{5}$$

$$\bar{\rho}\sqrt{\sigma}\,\frac{\partial}{\partial\bar{\phi}}\left(\frac{\sqrt{\sigma}\theta_{21}}{\bar{\rho}}\right) = \frac{1}{U^2}\left\{\Pi + M(0{\cdot}067\Lambda - 0{\cdot}669)\right\}. \tag{6}$$

In equation (6) we have

$$\Theta_{21} = -\int_0^\infty \frac{uv}{U^2}\,d\zeta = \theta_{21}\sqrt{(\sigma\nu)}, \tag{7}$$

and, as seen in Appendix I,

$$\theta_{21} = -\,p\Pi - mM, \tag{8}$$

where

$$p = 0{\cdot}2946 + 0{\cdot}0223\Lambda, \tag{9}$$

$$m = 0{\cdot}02983 + 0{\cdot}00380\Lambda. \tag{10}$$

Equation (5) is first solved by a quadrature. This determines σ and hence Λ and M by equation (3). Equation (6) is an equation for the parameter Π, since θ_{21} is given by equation (8) in terms of Π. It is best solved by a step-by-step procedure. Once Π_0 is known at any step an estimate for Π_1 is made for the next step. This determines $(\theta_{21})_1$ from equation (8). Equation (6) is now integrated by the trapezium rule, $(\theta_{21})_0$ being supposed known, and thus another value for $(\theta_{21})_1$ is found. If these do not agree a new estimate for Π is made and the process repeated. The method is quite easy and straightforward in practice, but it does require the interval to be small enough for the trapezium rule to be used.

Once σ and Π are known all properties of the boundary layer are known. Thus Θ_{11} and Θ_{21} are found from equation (4) and (7) above. The skin-friction components are given by

$$\tau_{01} = \mu\left(\frac{\partial u}{\partial\zeta}\right)_0 = \frac{\mu U}{\sqrt{(\sigma\nu)}}\,\frac{2}{3\sqrt{\pi}}\,(2+\Lambda), \tag{11}$$

$$\tau_{02} = \mu\left(\frac{\partial v}{\partial\zeta}\right)_0 = \frac{\mu U}{\sqrt{(\sigma\nu)}}\left(\Pi + \frac{2}{3\sqrt{\pi}}\,M\right), \tag{12}$$

as found in Appendix I, and from these we obtain

$$\tan\beta = \frac{\tau_{02}}{\tau_{01}} = \frac{(3\sqrt{\pi}/2)\Pi + M}{2+\Lambda} = \frac{2{\cdot}6587\Pi + M}{2+\Lambda}, \tag{13}$$

where β is the angle between streamlines and limiting streamlines.

In view of the comparison with exact results and with other methods as shown in Figs. 3, 4, 5 and 6, this is recommended as the standard method to use in general laminar flow. It follows closely the method of Zaat[2] as regards the streamwise flow though the cross-flow equation is quite different. Equation (6) contains the parameter Π instead of Zaat's parameter Ω. The new form is easier to integrate and does not need extensive tables of functions of Ω which the earlier form required.

It is to be understood that the integration is to be carried through along a streamline, or rather along a set of streamlines, one at a time.

Starting is often difficult and often occupies a large fraction of the total computing time. Fortunately it has been repeatedly found that the downstream solution is not at all sensitive to the way in which the solution started.

3. *The Choice of Test Example.*—It is necessary to make some choice out of the many possible in equations (1). In attached flow over slender wings at low incidences the streamlines are fairly straight, and as a rule there is over the surface a favourable pressure gradient to begin with, followed by a point of inflexion in the external streamlines and then an unfavourable pressure gradient. In an endeavour to reproduce these characteristics and yet retain as much simplicity as possible, the following external velocity was chosen.

$$\left.\begin{aligned} &U_1/U_0 = 1, \\ &V_1/U_0 = 2 + (x/c) - (x/c)^2, \quad \text{(Example I)} \end{aligned}\right\} \tag{14}$$

where U_0 is a representative velocity and c a representative length. This gives a family of streamlines having a point of inflexion at $x/c = 0{\cdot}5$. Streamlines and limiting streamlines for this system are shown in Fig. 2. It is surprising how much the very slight bending of the external streamlines downstream of the point of inflexion (and in the region of adverse pressure gradient) causes the limiting streamlines to bend. This seems to be a characteristic property of laminar flow over slender wings, and suggests that laminar separation is apt to take place a very short distance downstream of the point of inflexion, even though the curvature of the external streamlines is quite small.

This example was tested by all three approximate methods. As there may be some doubt as to the validity of the assumption of small cross-flow for very slender wings it was decided to use as a second example one which corresponds to a higher sweep, and so the value of V_1/U_0 in equation (14) was changed to

$$V_1/U_0 = 4 + 4(x/c) - 4(x/c)^2, \qquad \text{(Example II)}$$

making the simulated angle of sweep equal to 76 deg. Thirdly, as a matter of general interest it was thought worth while to try the method when the pressure gradient is originally unfavourable, changing to favourable downstream of the point of inflexion which remains at $x/c = 0{\cdot}5$ in all the examples. For this final test V_1/U_0 was given by

$$V_1/U_0 = 4 - 4(x/c) + 4(x/c)^2, \qquad \text{(Example III).}$$

A streamline and a limiting streamline for each of Examples II and III are shown in Figs. 7 and 11 respectively.

4. *The Exact Solution.*—We take Cartesian co-ordinates x, y in the plane surface $\zeta = 0$, and suppose that the velocity components in the direction of the axes are U_1 and V_1 outside the boundary layer. We suppose also that the velocity components along and perpendicular to the external streamlines are u and v.

We write

$$\bar{U}_1 = U_1/U_0, \qquad \bar{V}_1 = V_1/U_0, \qquad U = \sqrt{(U_1^2 + V_1^2)}, \qquad \bar{U} = U/U_0,$$

$$\bar{u} = u/U_0, \qquad \bar{v} = v/U_0, \qquad \bar{x} = x/c, \qquad \bar{y} = y/c.$$

The external velocity components may then be written

$$\left.\begin{aligned} \bar{U}_1 &= 1 \\ \bar{V}_1 &= \sum_{r=0}^{N'} a_r \bar{x}^r \end{aligned}\right\}. \tag{15}$$

Hansen and Herzig[1] show that

$$\bar{v} = \frac{1}{\bar{U}} \sum_{r=1}^{N'} a_r \bar{x}^r H_r(\eta), \tag{16}$$

$$\bar{u} = \bar{U} F'(\eta) + \bar{v}\bar{V}_1,$$

where

$$\eta = \zeta \left(\frac{U_0}{\nu x}\right)^{1/2},$$

and $F(\eta)$ (the Blasius function) and $H_r(\eta)$ are tabulated by them. Primes denote differentiation with respect to η.

The equation of the streamlines may be written

$$\bar{y} = \sum_{r=0}^{N'} \frac{a_r \bar{x}^{r+1}}{r+1} + \text{const},$$

and the equation of the limiting streamlines is

$$\bar{y} = \sum_{r=0}^{N'} \frac{a_r \bar{x}^{r+1}}{r+1} J_r(0) + \text{const}, \tag{17}$$

where $J_r(\eta)$ is tabulated by Hansen and Herzig[1].

If we denote by Θ_{11} the momentum thickness in the streamwise direction we have

$$\Theta_{11} = \int_0^\infty \frac{u}{\bar{U}}\left(1 - \frac{u}{\bar{U}}\right) d\zeta = \frac{1}{\bar{U}^2}\left(\frac{\nu x}{U_0}\right)^{1/2} \int_0^\infty \bar{u}(\bar{U} - \bar{u})\, d\eta.$$

Hence we have

$$\Theta_{11}\left(\frac{U_0}{\nu x}\right)^{1/2} \bar{U}^2 = 0{\cdot}66412\bar{U}^2 + \bar{V}_1 \sum_{r=1}^{N'} a_r \bar{x}^r \left(H_{r0} - 2H_{rf}\right) - \frac{\bar{V}_1^2}{\bar{U}^2} \sum_{r=1}^{N'} \sum_{s=1}^{N'} a_r a_s \bar{x}^r \bar{x}^s H_{rs},$$

where

$$H_{r0} = \int_0^\infty H_r \, d\eta, \qquad H_{rf} = \int_0^\infty H_r F' \, d\eta, \qquad H_{rs} = \int_0^\infty H_r H_s \, d\eta, \tag{18}$$

and the coefficient of $\bar{U}^2$ comes from the result

$$\int_0^\infty F' (1 - F') \, d\eta = 0{\cdot}66412.$$

The skin friction in the streamwise direction, denoted by τ_{01}, is given by

$$\begin{aligned} \tau_{01} &= \mu \left(\frac{\partial u}{\partial \zeta}\right)_0 = \mu U_0 \left(\frac{U_0}{\nu x}\right)^{1/2} \left(\frac{\partial \bar{u}}{\partial \eta}\right)_0 \\ &= \mu U_0 \left(\frac{U_0}{\nu x}\right)^{1/2} \left\{ \bar{U} F''(0) + \frac{\bar{V}_1}{\bar{U}} \sum_{r=1}^{N'} a_r \bar{x}^r H_r'(0) \right\}. \end{aligned}$$

Hence we have

$$\frac{\tau_{01}}{\mu \bar{U}} \left(\frac{\nu x}{U_0}\right)^{1/2} = 0{\cdot}33206 + \frac{\bar{V}_1}{\bar{U}^2} \sum_{r=1}^{N'} a_r \bar{x}^r H_r'(0).$$

The skin friction at right angles to the streamlines, denoted by τ_{02}, may be found in a similar way. We have

$$\frac{\tau_{02}}{\mu U_0} \left(\frac{\nu x}{U_0}\right)^{1/2} \bar{U} = \sum_{r=1}^{N'} a_r \bar{x}^r H_r'(0).$$

If β is the angle between the limiting streamlines and the external streamlines we have

$$\cot \beta = \frac{\tau_{01}}{\tau_{02}} = \bar{V}_1 + \frac{0{\cdot}33206 \bar{U}^2}{\sum_{r=1}^{N'} a_r \bar{x}^r H_r'(0)}.$$

By numerical integration from the results of Ref. 1 we find that

$$H_{10} = 1{\cdot}6106, \qquad H_{20} = 2{\cdot}2750, \qquad H_{11} = 0{\cdot}7558,$$

$$H_{12} = 1{\cdot}0918, \qquad H_{22} = 1{\cdot}5892,$$

and it can be shown that

$$H_{1f} = 0{\cdot}8659, \qquad H_{2f} = 1{\cdot}1619.$$

From the Tables of Ref. 1 we also have

$$H_1'(0) = 1{\cdot}0860, \qquad H_2'(0) = 1{\cdot}8651.$$

Thus the main properties of the boundary layer may be obtained in a straightforward way.

For this particular example the basic method of solution outlined in Section 2 must be slightly modified. It is only a modification of detail, not a change of method, and is due to the fact that the external flow is not irrotational and so a velocity potential does not exist. This modification is carried out in Appendix III.

5. *The Recommended Method of Solution in the Special Case.*—In this case we take

$$\bar{U}_1 = 1, \quad \bar{V}_1 = \sum_{r=1}^{N'} a_r \bar{x}^r,$$

and by Appendix III, equation (39) we find σ from the equation

$$\frac{\sigma U_0}{c} = \frac{5{\cdot}08}{\bar{U}^4} \int_0^x \bar{U}^4 \, d\bar{x} = \frac{5{\cdot}08}{\bar{U}^4} \int_0^{\bar{x}} \left\{ 1 + \left(\sum a_r \bar{x}^r \right)^2 \right\}^2 d\bar{x} \, . \tag{19}$$

The integral may be immediately evaluated since the integrand is a polynomial.

We determine Π from equation (40), that is,

$$\frac{d}{d\bar{x}} \left\{ \left(\frac{\sigma U_0}{c} \right)^{1/2} \theta_{21} \right\} = \left(\frac{\sigma U_0}{c} \right)^{-1/2} \left\{ \Pi + M(0{\cdot}067\Lambda - 0{\cdot}669) \right\},$$

where

$$\Lambda = \frac{\sigma U_0}{c} \frac{\bar{V}_1}{\bar{U}^2} \frac{d\bar{V}_1}{d\bar{x}}, \qquad M = -\frac{\Lambda}{\bar{V}_1},$$

and θ_{21} is given by equations (8), (9) and (10). When σ and Π are found the other properties of the boundary layer are obtained from equations (4), (11), (12) and (13).

6. *Discussion of the Results.*—Figs. 3, 4, 5 and 6 give respectively the streamwise momentum thickness, streamwise skin friction, cross-flow skin friction and angle between streamlines and limiting streamlines for Example I as calculated by various methods. These are compared with their exact values.

Θ_{11} and τ_{01} are unchanged in Zaat's two methods, but τ_{02} and β are different. In these cases, in Figs. 5 and 6 the earlier method[3] is denoted by 'Zaat (1)' and the later method[11, 12] by 'Zaat (2)'. It will be seen that the later method gives some improvement on the earlier one, but the main source of error in both seems to be the parameter N, introduced originally in order to produce a streamwise 'separation profile' in the two-dimensional sense. This may not be necessary as, in general, three-dimensional separation is not singular and does not require the vanishing of the streamwise skin friction. In any case all the methods probably break down when separation is approached, which will usually be at a place where the cross-flow is not small. The effect of N is to make τ_{01} far too small. If N were dropped the curve for τ_{01} by Zaat's method would become identical with that marked 'present method' in Fig.4. That for τ_{02} would be hardly changed at all, but tan β would be greatly improved.

It will be seen that the recommended method gives the greatest accuracy and will give reasonably close results up to an angle β of 15 deg. This may be sufficient for slender wings, as it seems likely that for angles greater than this the boundary layer may separate or become turbulent. Strong cross-flow is known to promote instability. The method may be adequate for the rough determination of separation, as this usually occurs when the limiting streamlines are turning rapidly.

Examples II and III compare only the recommended method with the exact solution. Example II, illustrated in Figs. 7, 8, 9 and 10, suggests that increased sweep may not noticeably affect the earlier conclusions. The errors in Example III are greater than the others in the earlier stages, but show a tendency to correct themselves. On the whole one may infer that the method is quite good at the start, even for adverse pressure gradients, and continues quite good downstream so long as the pressure gradient is favourable. When the limiting streamlines turn considerably the method ceases to be of value (as is to be expected in view of the violation of the basic assumption of small cross-flow), but it may still forecast separation if the latter occurs abruptly enough.

All the methods used resemble each other for the streamwise flow. They all involve a simple quadrature to find the momentum thickness, but then vary slightly in the determination of other streamwise properties.

For the cross-flow the order of increasing complexity is first, Eichelbrenner and Oudart's method, second, the present recommended method, and third, Zaat's method. The last two require the numerical solution of a differential equation in which the interval must be taken sufficiently small for the trapezium rule to be used.

We give one more example, calculated by all three methods, in which the exact solution is not known. It is for a conically cambered thin delta wing from Ref. 10, with attached flow along the leading edges. The angle of sweep is 72 deg. The calculations by Zaat's method were done in Ref. 9. In Fig. 15 is shown the angle between the limiting streamlines and rays, calculated by the three methods. Separation takes place at the point where this angle vanishes. In this Figure η is defined by the equation

$$\eta = (y/x) \tan 72°,$$

where the axis of x is taken along the centre-line of the wing and that of y is perpendicular to it. It will be seen that separation takes place at $\eta = 0{\cdot}625$, $0{\cdot}645$ and $0{\cdot}690$ for the three methods. From this it can be calculated that separation is along rays making angles $11{\cdot}5$, $11{\cdot}8$ and $12{\cdot}7$ deg with the centre-line. The leading edge makes an angle of 18 deg with the centre-line.

Compared with the present method Zaat's method gives a slightly early separation line, whilst Eichelbrenner and Oudart's method gives separation earlier still. At separation the angle β between streamlines and limiting streamlines is about 16 deg. For this example separation occurs very early, and as a result the external and boundary-layer parts of the flow cannot match. In Ref. 9 a calculation was done by Zaat's method for a different cambered wing in which $\bar{\eta} = 0$. For this example we show in Figs. 16a and 16b a streamline and a limiting streamline. This illustrates the type of streamline to be expected on slender wings with attached flow, though strictly, as before, the internal and external flows do not match, though the discrepancy is less marked here.

7. *Conclusions.*—From the examples tested all three methods give a reasonable picture of the flow, displaying all its main features. The present recommended method, which does not involve excessive

computing time, gives quite an accurate solution so long as the limiting streamlines do not diverge in direction greatly from that of the external streamlines. All the methods require the use of streamline co-ordinates, which are sometimes laborious to compute, but it seems well established that any method will require this preliminary work.

The tests give grounds for hope that the recommended method may be acceptable to quite reasonable accuracy in an accelerated flow and in the earlier part of retarded flow; it may even be hoped that it will predict separation without gross inaccuracy.

LIST OF SYMBOLS

a_r		Coefficient of x^r in equation (1)
c		A reference length
$f(z)$, $g(z)$, $h(z)$, $\bar{h}(z)$		Velocity profiles defined by equations (2), (21) and (22)
$F(\eta)$		The Blasius function (Ref. 1)
$H(\eta)$		Defined by equation (16) (*See* Ref. 1)
h_1, h_2		Defined by equation (26). Coefficients in line element
H_{r0}, H_{rj}, H_{rs}		Defined by equation (18)
$H(\Delta)$		Defined by equation (34)
$J_r(0)$		Defined by equation (17) (*See* Ref. 1)
m		Defined by equation (10)
N'		Highest power of x occurring in equation (1)
N		Defined by equation (22)
p		Defined by equation (9)
T	$=$	$\left(U_1^2 + V_1^2\right)^{1/2}$
u, v		Velocity components in the boundary layer along and perpendicular to the external streamlines
$\bar{u}$, $\bar{v}$	$=$	u/U_0, v/U_0
U, V		In Appendix II. External velocity components parallel to the co-ordinate curves
U_0	$=$	A reference velocity
U	$=$	Resultant external velocity (along a streamline) (except in early part of Appendix II)
U_1, V_1		External velocity components along the axes of x and y
$\bar{U}_1$, $\bar{V}_1$	$=$	U_1/U_0, V_1/U_0
x, y, ζ		Cartesian co-ordinates
$\bar{x}$, $\bar{y}$	$=$	x/c, y/c
z	$=$	$\zeta(\sigma\nu)^{-1/2}$
β		Angle between external streamlines and limiting streamlines
Δ_1, Δ_2		Displacement-thickness 'components'
δ_1		Defined by equations (33)

$\Theta_{11}, \Theta_{12}, \Theta_{21}, \Theta_{22}$		Momentum-thickness 'components'
θ_{11}, θ_{21}		Defined by equations (33)
ζ		Distance from the surface
η	$=$	$\zeta\left(U_0/\nu x\right)^{1/2}$
K		Velocity profile parameter
A		Velocity profile parameter
M		Velocity profile parameter
μ		Coefficient of viscosity
ν		Kinematic viscosity
Π		Velocity profile parameter
ρ_1, ρ_2		Defined by $h_1^2 = 1/\rho_1 U^2$, $h_2^2 = 1/\rho_2 U^2$
$\bar{\rho}$		Form for ρ_2 when $\rho_1 = 1$
σ		Parameter related to boundary-layer thickness
τ_{01}, τ_{02}		Skin-friction components
ϕ		Function behaving like a velocity potential
ψ		Function behaving like a stream function
Ω		Velocity profile parameter used in Refs. 3 and 5

LIST OF REFERENCES

No.	*Author*	*Title, etc.*
1	A. G. Hansen and H. Z. Herzig ..	Cross-flows in laminar incompressible boundary layers. N.A.C.A. Tech. Note 3651. February, 1956. Also: Experimental and analytical investigation of flow in ducts. *J. Ae. Sci.* Vol. 24. p. 217. 1957.
2	E. A. Eichelbrenner and A. Oudart	Mêthode de calcul de la couche limite tridimensionnelle. Application à un corps fusilé incliné sur le vent. O.N.E.R.A. Publication 76. April, 1955.
3	J. A. Zaat	A simplified method for the calculation of three-dimensional laminar boundary layers. N.L.L. Report F184. April, 1956.
4	R. Timman	A one-parameter method for the calculation of laminar boundary layers. N.L.L. Report F35. 1948.
5	R. Timman	The theory of three-dimensional boundary layers. Proceedings of a Symposium on Boundary Layer Effects in Aerodynamics held at the N.P.L. 1955.
6	R. Timman	A calculation method for three-dimensional laminar boundary layers. N.L.L. Report F66. August, 1950.
7	W. Mangler	Zusammenhang zwischen ebenen und rotationssymmetrischen Grenzschichten in kompressiblen Flüssigkeiten. *Z.A.M.M.* Vol. 28, p. 97. 1948.
8	B. Thwaites	Approximate calculation of the laminar boundary layer. *Aero. Quart.* Vol. 1. p. 245. 1949.
9	J. C. Cooke	An approximate method of calculating the laminar boundary layer on a delta wing. A.R.C. 20,996. November, 1958.
10	G. G. Brebner	Some simple conical camber shapes to produce low lift dependent drag on a slender delta wing. C.P. 428. September, 1957.
11	J. A. Zaat	Nachprüfung der einfachen Rechenmethode für dreidimensionale laminare Grenzschichten mit Hilfe von exakten Lösungen. N.L.L. Report F202. June, 1957.
12	J. A. Zaat	Das Verhalten der dreidimensionalen, laminanen Grenzschichströmung bei zunehmenden Anstellwinkeln. N.L.L. Tech. Note F215. May, 1958.

APPENDIX I

The Velocity Profiles

We take

$$\frac{u}{U} = f(z) - \Lambda g(z), \tag{20}$$

$$\frac{v}{U} = \Pi h(z) - M g(z), \tag{21}$$

where Λ and M are parameters given in equation (3), while Π is a third parameter to be determined.

Other functions are defined by

$$\zeta = \sqrt{(\sigma\nu)}\, z,$$

$$1 - f(z) = 2g(z) + e^{-z^2}$$

$$= \frac{2}{3\sqrt{\pi}} z\, e^{-z^2} + \frac{2}{\sqrt{\pi}} \int_z^\infty e^{-t^2}\, dt,$$

$$h(z) = z\, e^{-z^2}.$$

Although we do not use them here we give for completeness Timman's and Zaat's profiles. The former are

$$\frac{u}{U} = f(z) - \Lambda g(z) - N\bar{h}(z), \tag{22}$$

$$\frac{v}{U} = -\Omega^2 M g\left(\frac{z}{\Omega}\right),$$

where $N = 0$ if $\Lambda \geqslant 0$, $N = \Lambda$ if $\Lambda < 0$, and Ω is a parameter relating the thicknesses of the streamwise and cross-flow boundary layers.

Zaat's later method [11, 12] replaces Timman's equation for v/U by

$$\frac{v}{U} = -\Omega^2 M g\left(\frac{z}{\Omega}\right) + \Omega^2 K \bar{h}\left(\frac{z}{\Omega}\right),$$

where

$$2\bar{h}(z) = 1 - f(z) - (1 + z^2)\, e^{-z^2},$$

and K is a new parameter. Zaat puts $K = 0$ until the point of inflexion is approached. After some point not completely specified (beyond the fact that it is somewhere upstream of the point of inflexion of the external streamline) he keeps Ω constant at the value it has now reached, and varies K, starting at $K = 0$, continuing until K once more becomes zero. At this point K is again kept zero and Ω is allowed to vary once more.

Timman shows that for the profiles (20) and (21)

$$\delta_1 = \int_0^\infty \left(1 - \frac{u}{U}\right) dz = 0{\cdot}752253 - 0{\cdot}066987\Lambda, \tag{23}$$

$$\theta_{21} = -\int_0^\infty \frac{u}{U}\frac{v}{U}\, dz = -p\Pi - mM,$$

where

$$p = 0{\cdot}294628 + 0{\cdot}022314\Lambda,$$

$$m = 0{\cdot}029826 + 0{\cdot}0037975\Lambda,$$

$$\theta_{11} = \int_0^\infty \frac{u}{U}\left(1 - \frac{u}{U}\right) dz = 0{\cdot}289430 + 0{\cdot}007335\Lambda - 0{\cdot}003798\Lambda^2.$$

We have at $z = 0$

$$f = g = h = f'' = f''' = g''' = f'''' = 0,$$

$$f' = -2g' = \frac{4}{3\sqrt{\pi}}, \qquad h' = 1, \qquad h'' = 0, \qquad g'' = 1.$$

This gives

$$\frac{1}{U}\left(\frac{\partial u}{\partial z}\right)_{z=0} = \frac{2}{3\sqrt{\pi}}(2 + \Lambda) = 0{\cdot}376127(2 + \Lambda) \quad \ldots \tag{24}$$

$$\frac{1}{U}\left(\frac{\partial v}{\partial z}\right)_{z=0} = \Pi + \frac{2}{3\sqrt{\pi}} M = 0{\cdot}376127(2{\cdot}65868\Pi + M). \tag{25}$$

APPENDIX II

Derivation of the Equations

In a co-ordinate system ζ, η, ζ whose line element is given by

$$ds^2 = h_1^2\,d\xi^2 + h_2^2\,d\eta^2 + d\zeta^2, \tag{26}$$

where ζ is distance measured normal to the surface, Timman[5] has shown that the boundary-layer equations in incompressible flow may be written

$$\frac{1}{h_1}\left(U\frac{\partial U}{\partial \xi} - u\frac{\partial u}{\partial \xi}\right) + \frac{1}{h_2}\left(V\frac{\partial U}{\partial \eta} - v\frac{\partial u}{\partial \eta}\right) - w\frac{\partial u}{\partial \zeta} +$$

$$+\left(UV - uv\right)\frac{1}{h_1 h_2}\frac{\partial h_1}{\partial \eta} - \left(V^2 - v^2\right)\frac{1}{h_1 h_2}\frac{\partial h_2}{\partial \xi} = -\nu\frac{\partial^2 u}{\partial \zeta^2}, \tag{27}$$

$$\frac{1}{h_1}\left(U\frac{\partial V}{\partial \xi} - u\frac{\partial v}{\partial \xi}\right) + \frac{1}{h_2}\left(V\frac{\partial V}{\partial \eta} - v\frac{\partial v}{\partial \eta}\right) - w\frac{\partial v}{\partial \zeta} -$$

$$-\left(U^2 - u^2\right)\frac{1}{h_1 h_2}\frac{\partial h_1}{\partial \eta} + \left(UV - uv\right)\frac{1}{h_1 h_2}\frac{\partial h_2}{\partial \xi} = -\nu\frac{\partial^2 v}{\partial \zeta^2}. \tag{28}$$

In these equations U and V are external velocity components parallel to the co-ordinate curves. The corresponding momentum equations are also given by Timman[5]. They take the form

$$\frac{1}{h_1}\frac{\partial \Theta_{11}}{\partial \xi} + \frac{1}{h_2}\frac{\partial \Theta_{12}}{\partial \eta} + \frac{2}{h_1 T}\frac{\partial T}{\partial \xi}\Theta_{11} + \frac{2}{h_2 T}\frac{\partial T}{\partial \eta}\Theta_{12} + \frac{1}{h_1 T}\frac{\partial U}{\partial \xi}\Delta_1 + \frac{1}{h_2 T}\frac{\partial U}{\partial \eta}\Delta_2 +$$

$$+\frac{1}{h_1 h_2}\frac{\partial h_2}{\partial \xi}\left(\Theta_{11} - \Theta_{22} - \frac{V}{T}\Delta_2\right) + \frac{1}{h_1 h_2}\frac{\partial h_1}{\partial \eta}\left(\Theta_{12} + \Theta_{21} + \frac{V}{T}\Delta_1\right) = \frac{\nu}{T^2}\left(\frac{\partial u}{\partial \zeta}\right)_0, \tag{29}$$

$$\frac{1}{h_2}\frac{\partial \Theta_{22}}{\partial \eta} + \frac{1}{h_1}\frac{\partial \Theta_{21}}{\partial \xi} + \frac{2}{h_2 T}\frac{\partial T}{\partial \eta}\Theta_{22} + \frac{2}{h_1 T}\frac{\partial T}{\partial \xi}\Theta_{21} + \frac{1}{h_2 T}\frac{\partial V}{\partial \eta}\Delta_2 + \frac{1}{h_1 T}\frac{\partial V}{\partial \xi}\Delta_1 +$$

$$+\frac{1}{h_1 h_2}\frac{\partial h_1}{\partial \eta}\left(\Theta_{22} - \Theta_{11} - \frac{U}{T}\Delta_1\right) + \frac{1}{h_1 h_2}\frac{\partial h_2}{\partial \xi}\left(\Theta_{21} + \Theta_{12} + \frac{U}{T}\Delta_2\right) = \frac{\nu}{T^2}\left(\frac{\partial v}{\partial \zeta}\right)_0, \tag{30}$$

where

$$T^2 = U^2 + V^2,$$

$$\Delta_1 T = \int_0^\infty (U - u)\,d\zeta, \qquad \Delta_2 T = \int_0^\infty (V - v)\,d\zeta,$$

$$\Theta_{11}T^2 = \int_0^\infty (U - u)u\,d\zeta, \qquad \Theta_{12}T^2 = \int_0^\infty (U - u)v\,d\zeta,$$

$$\Theta_{21}T^2 = \int_0^\infty (V - v)u\,d\zeta, \qquad \Theta_{22}T^2 = \int_0^\infty (V - v)v\,d\zeta.$$

It should be noted that the definition of T given here is different from that of Timman[5].

We introduce streamline co-ordinates so that the line element ds on the surface is given by

$$ds^2 = \frac{d\phi^2}{\rho_1 U^2} + \frac{d\psi^2}{\rho_2 U^2}.$$

We again differ slightly here from Timman because we wish to be able to consider rotational flows for which a velocity potential does not exist. Nevertheless, surface streamlines $\psi = \text{const.}$ and their surface orthogonal trajectories $\phi = \text{const.}$ still exist in general. The point is that the co-ordinates are 'streamline' co-ordinates and we must now have

$$V = 0, \qquad T = U,$$

and U is the resultant velocity along the streamlines.

If we use the velocity profiles (20) and (21) of Appendix I, with $\zeta = (\sigma\nu)^{1/2}z$, equations (27) and (28) provide us with boundary conditions on the surface $\zeta = 0$. We put $u = v = w = 0$, $V = 0$ in the equations, and we find on putting $h_1 = 1/U\sqrt{\rho_1}$, $h_2 = 1/U\sqrt{\rho_2}$, $V = 0$, $T = U$, and using the co-ordinates ϕ and ψ,

$$\Lambda = \sqrt{\rho_1}\,\sigma\, U \frac{\partial U}{\partial \phi}, \tag{31}$$

$$M = \sqrt{\rho_2}\,\sigma\, U\left[\frac{\partial U}{\partial \psi} + \frac{U}{2\rho_1}\frac{\partial \rho_1}{\partial \psi}\right]. \tag{32}$$

We now make the assumption that v, the cross-flow, is small in the equations (29) and (30). Writing

$$\left.\begin{aligned} \delta_1 &= \int_0^\infty \left(1 - \frac{u}{U}\right) dz, \qquad & \theta_{11} &= \int_0^\infty \frac{u}{U}\left(1 - \frac{u}{U}\right) dz, \\ & & \theta_{21} &= -\int_0^\infty \frac{uv}{U^2}\, dz, \end{aligned}\right\} \tag{33}$$

and using equations (24) and (25) we obtain

$$\sqrt{\rho_1}\left\{\frac{\partial}{\partial\phi}\left(\sqrt{\sigma}\theta_{11}\right) + \frac{\sqrt{\sigma}}{U}\frac{\partial U}{\partial\phi}\left(\theta_{11} + \delta_1\right) - \frac{\sqrt{\sigma}}{2\rho_2}\frac{\partial\rho_2}{\partial\phi}\theta_{11}\right\} = \frac{1}{\sqrt{\sigma}U^2}\,\frac{2}{3\sqrt{\pi}}(2 + \Lambda),$$

$$\sqrt{\rho_1}\frac{\partial}{\partial\phi}\left(\sqrt{\sigma}\theta_{21}\right) - \frac{\sqrt{(\rho_1\sigma)}}{\rho_2}\frac{\partial\rho_2}{\partial\phi}\theta_{21} + \sqrt{(\rho_2\sigma)}\left(\frac{1}{U}\frac{\partial U}{\partial\psi} + \frac{1}{2\rho_1}\frac{\partial\rho_1}{\partial\psi}\right)\left(\theta_{11} + \delta_1\right)$$

$$= \frac{1}{\sqrt{\sigma}U^2}\left(\Pi + \frac{2}{3\sqrt{\pi}}M\right).$$

Using equations (31) and (32) and rearranging we obtain

$$\sqrt{\rho_1}\,\rho_2\frac{\partial}{\partial\phi}\left(\frac{U^2\sigma\theta_{11}^2}{\rho_2}\right) = \frac{4}{3\sqrt{\pi}}\,\theta_{11}(2 + \Lambda) - 2\Lambda\theta_{11}\delta_1 \equiv H(\Lambda), \tag{34}$$

$$\frac{\rho_2^2\sqrt{\rho_1}}{2\theta_{21}}\frac{\partial}{\partial\phi}\left(\frac{\sigma\theta_{21}^2}{\rho_2^2}\right)=\frac{1}{U^2}\left\{\Pi+M\left(\frac{2}{3\sqrt{\pi}}-\theta_{11}-\delta_1\right)\right\}, \tag{35}$$

as may be verified directly.

Now we may put approximately

$$\theta_{11}=a=0{\cdot}293, \qquad H(\Lambda)=0{\cdot}436-2a^2\Lambda, \tag{36}$$

as Zaat does. Fig. 17 shows that these approximations give reasonable accuracy in the range $1>\Lambda>-0{\cdot}8$ which seems to be sufficient.

Equation (34) then reduces to

$$\sqrt{\rho_1}\frac{\partial}{\partial\phi}\left(\frac{U^4\sigma}{\rho_2}\right)=5{\cdot}08\frac{U^2}{\rho_2}, \tag{37}$$

whilst equation (35) becomes

$$\begin{aligned}\rho_2\sqrt{(\rho_1\sigma)}\frac{\partial}{\partial\phi}\left(\frac{\sqrt{\sigma}\theta_{21}}{\rho_2}\right)&=\frac{1}{U^2}\left\{\Pi+M\left(\frac{2}{3\sqrt{\pi}}-a-\delta_1\right)\right\}\\&=\frac{1}{U^2}\left\{\Pi+M(0{\cdot}067\Lambda-0{\cdot}669)\right\},\end{aligned} \tag{38}$$

using the values of a and δ_1 from equations (36) and (23).

APPENDIX III

Equations in the Special Case

If the external flow is of the form given in equation (15) a velocity potential does not exist. However, a stream function ψ exists in the sense that a ψ can be found such that

$$\frac{\partial \psi}{\partial x} = V_1 = U_0 \bar{V}_1 = U_0 \sum_{r=0}^{N'} a_r \bar{x}^r, \qquad \frac{\partial \psi}{\partial y} = -U_1 = -U_0.$$

We may therefore take the streamline co-ordinate

$$\psi = cU_0 \left\{ \sum_{r=0}^{N'} \frac{a_r \bar{x}^{r+1}}{r+1} - \bar{y} \right\}.$$

We find also that we may take the other streamline co-ordinate

$$\phi = cU_0 \left\{ \int \frac{d\bar{x}}{\bar{V}_1} + \bar{y} \right\},$$

since these give

$$ds^2 = dx^2 + dy^2 = \frac{\bar{V}_1^2 \, d\phi^2}{U^2} + \frac{d\psi^2}{U^2}.$$

This form shows that the system is orthogonal as required, but ϕ is not a velocity potential. Hence we have

$$\rho_1 = \frac{1}{\bar{V}_1^2}, \qquad \rho_2 = 1.$$

We also have, when ϕ is constant

$$\frac{d\bar{x}}{\bar{V}_1} + d\bar{y} = 0,$$

and, when this equation holds,

$$d\psi = cU_0 (\bar{V}_1 \, d\bar{x} - d\bar{y})$$

$$= cU_0 \frac{1 + \bar{V}_1^2}{\bar{V}_1} \, d\bar{x},$$

and so, when ϕ is constant

$$\frac{\partial}{\partial \psi} = \frac{1}{cU_0} \frac{\bar{V}_1}{U^2} \frac{d}{d\bar{x}},$$

noting that

$$\bar{U}^2 = 1 + \bar{V}_1^2.$$

In a similar way we can show that, when ψ is constant,

$$\frac{\partial}{\partial \phi} = \frac{1}{cU_0} \frac{\bar{V}_1}{\bar{U}^2} \frac{d}{d\bar{x}}.$$

Hence we find from equations (31) and (32)

$$\Lambda = \frac{\sigma U_0}{c} \frac{\bar{V}_1}{\bar{U}^2} \frac{d\bar{V}_1}{d\bar{x}}, \qquad M = -\frac{\Lambda}{\bar{V}_1}.$$

Now equation (37) becomes

$$\frac{d}{d\bar{x}} \left(\frac{\sigma U_0}{c} \bar{U}^4 \right) = 5{\cdot}08 \bar{U}^4,$$

and hence

$$\frac{\sigma U_0}{c} = \frac{5{\cdot}08}{\bar{U}^4} \int_0^{\bar{x}} \bar{U}^4 \, d\bar{x}, \tag{39}$$

since $\sigma = 0$ at the start as can be seen from the exact solution.

Equation (38) becomes

$$\frac{d}{d\bar{x}} \left\{ \sqrt{\left(\frac{\sigma U_0}{c} \right)} \theta_{21} \right\} = \frac{1}{\sqrt{(\sigma U_0/c)}} \left\{ \Pi + M(0{\cdot}067\Lambda - 0{\cdot}669) \right\}. \tag{40}$$

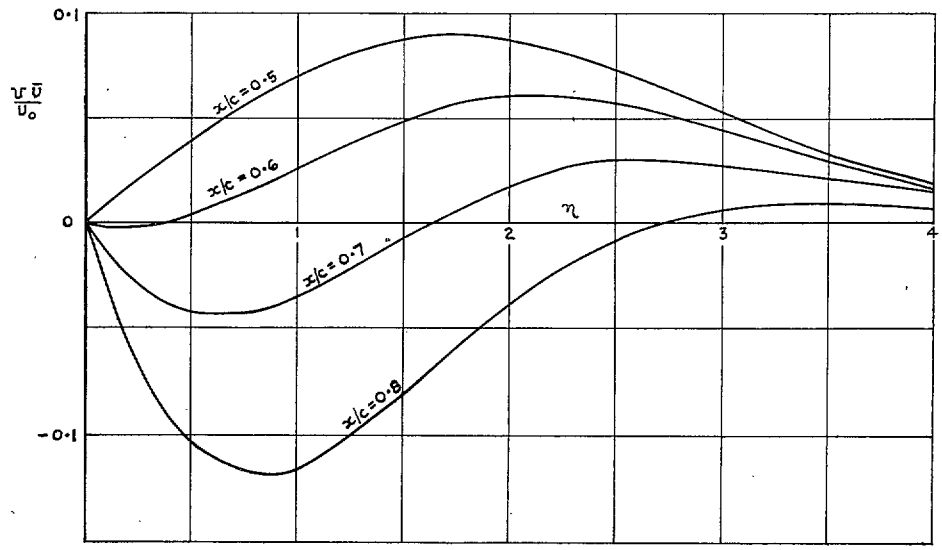

FIG. 1. Cross-flow velocity profiles. External point of inflexion at $x/c = 0{\cdot}5$. Example I. Exact.

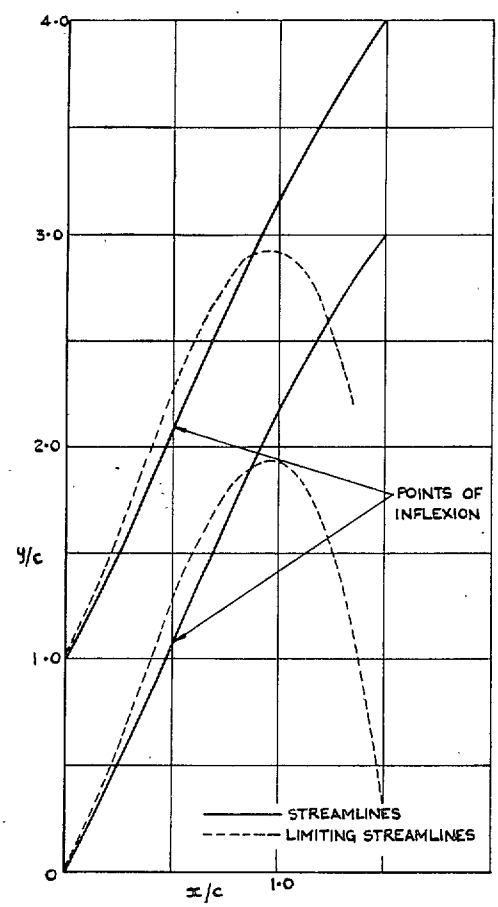

FIG. 2. Streamlines and limiting streamlines. Example I. Exact.

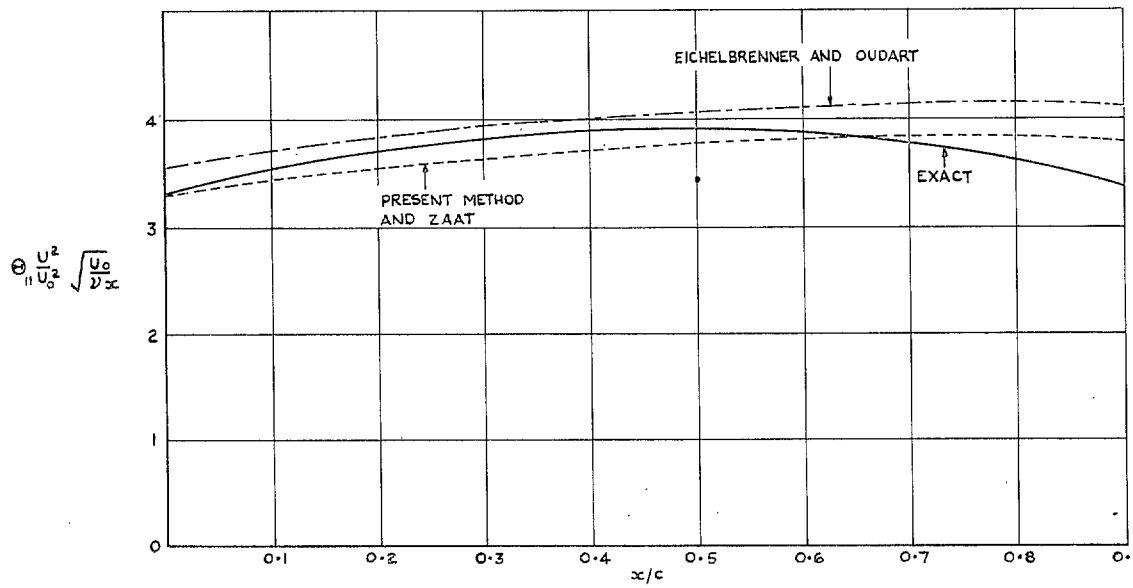

FIG. 3. Momentum thickness. Example I.

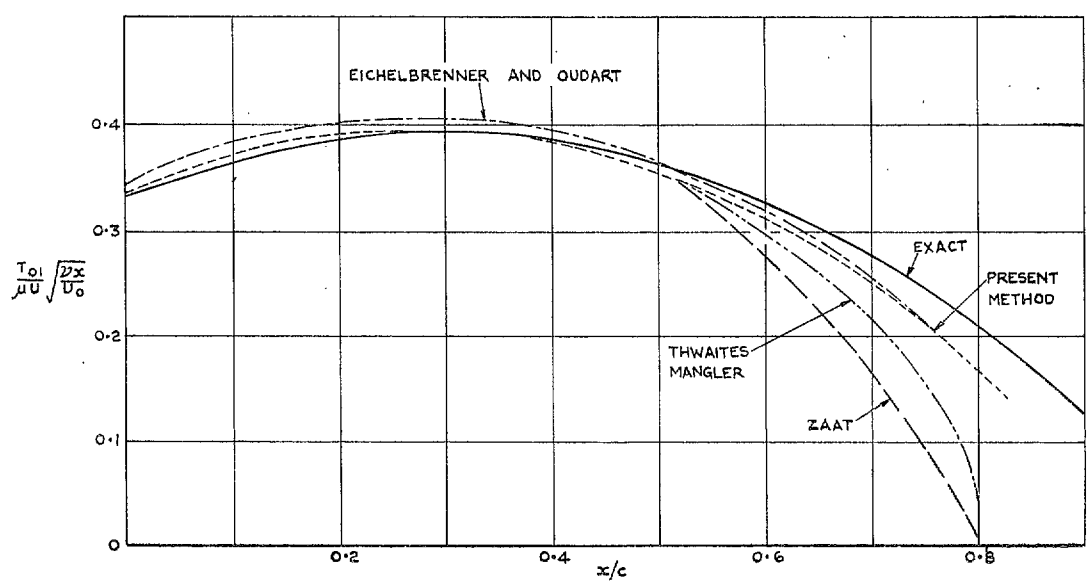

FIG. 4. Streamwise skin friction. Example I.

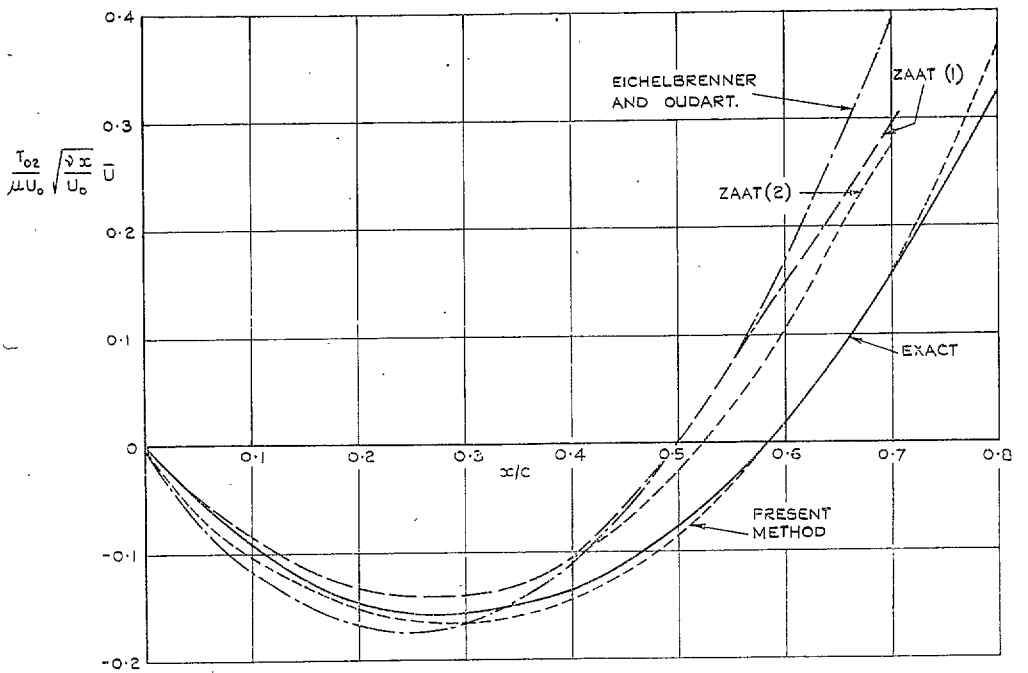

FIG. 5. Cross-flow skin friction. Example I.

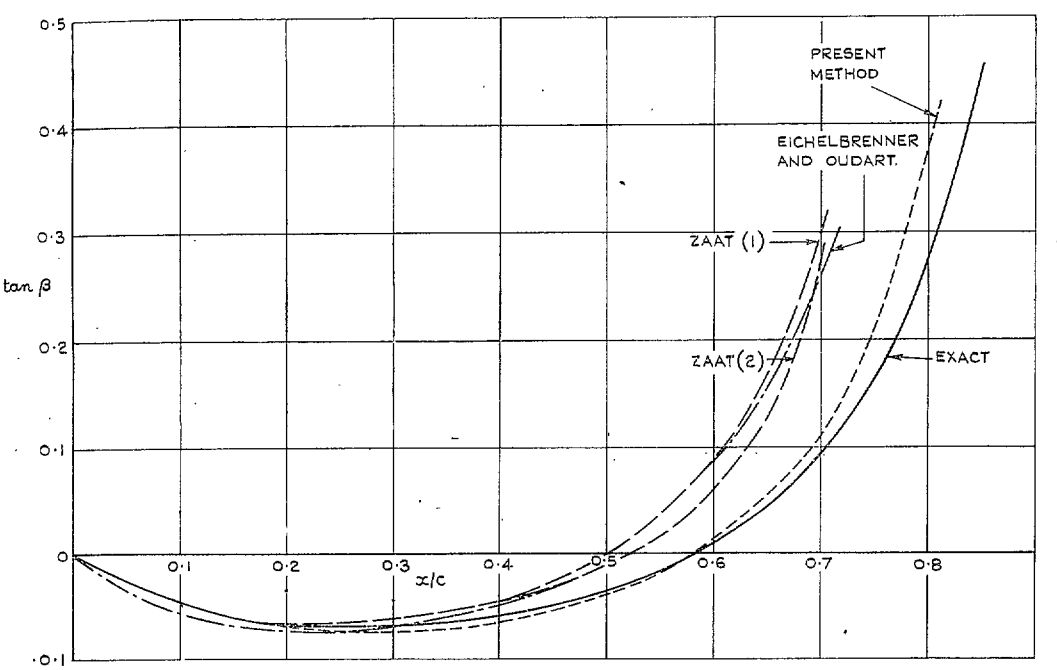

FIG. 6. Values of tan β, where β is the angle between streamlines and limiting streamlines. Example I.

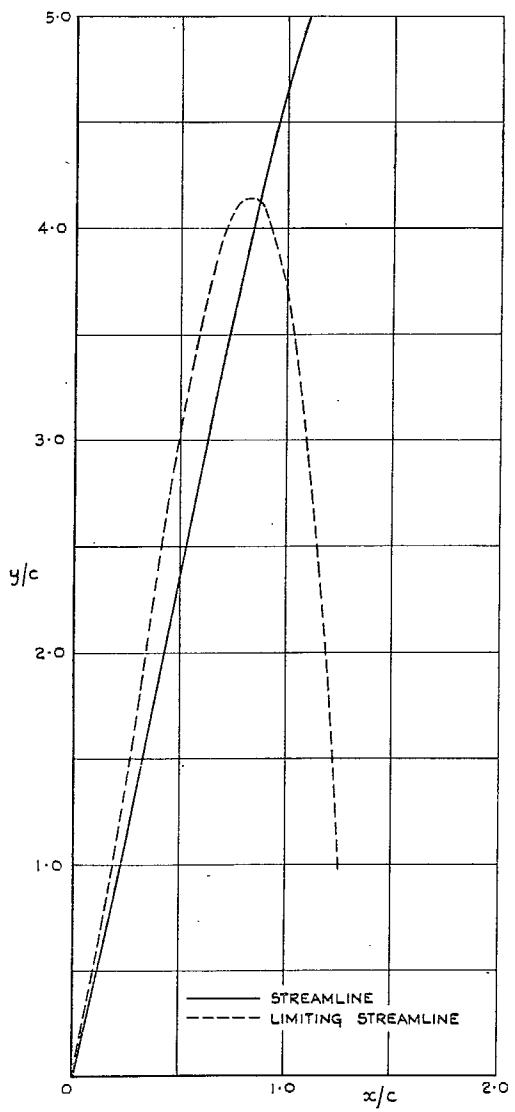

FIG. 7. Streamline and limiting streamline. Example II. Exact.

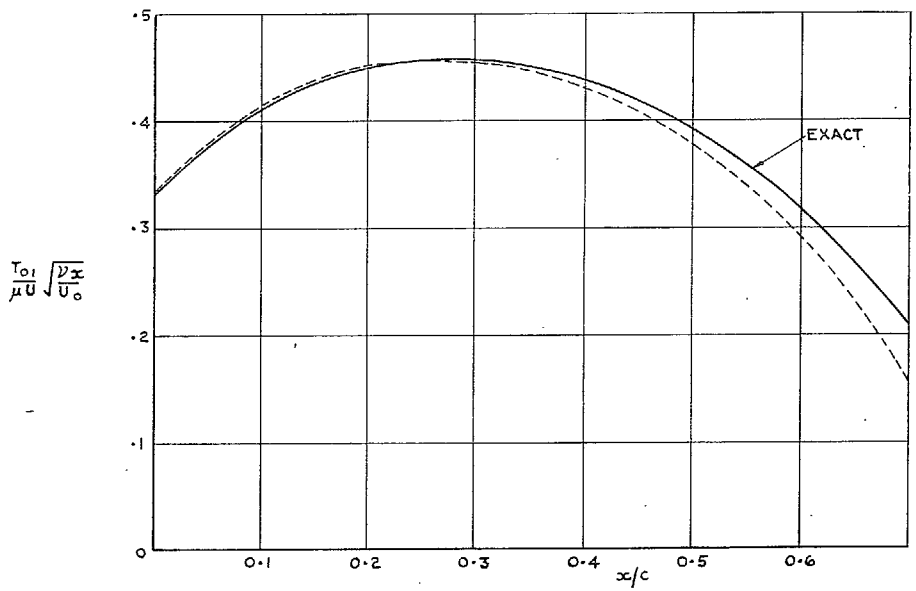

FIG. 8. Streamwise skin friction. Example II.

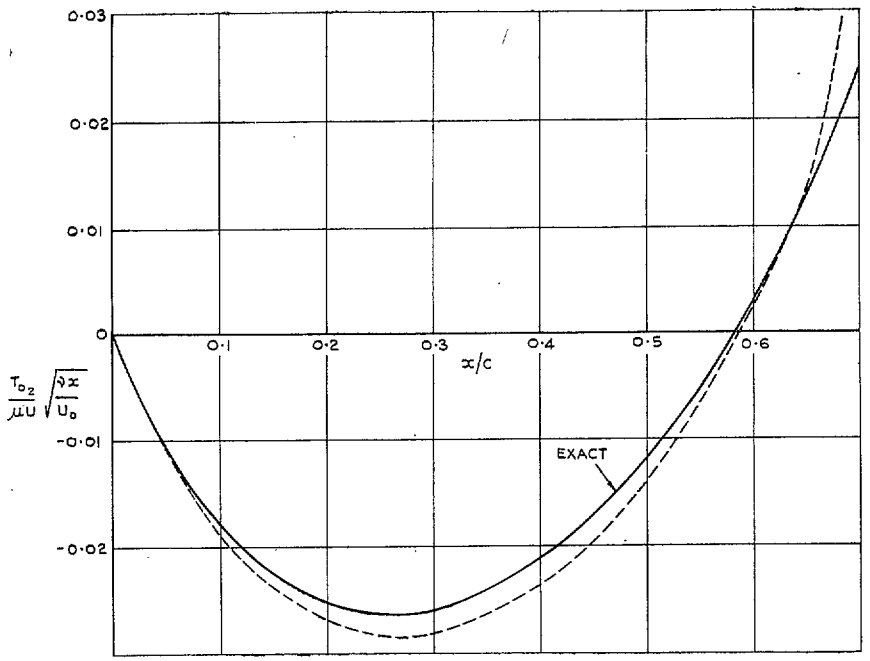

FIG. 9. Cross-flow skin friction. Example II.

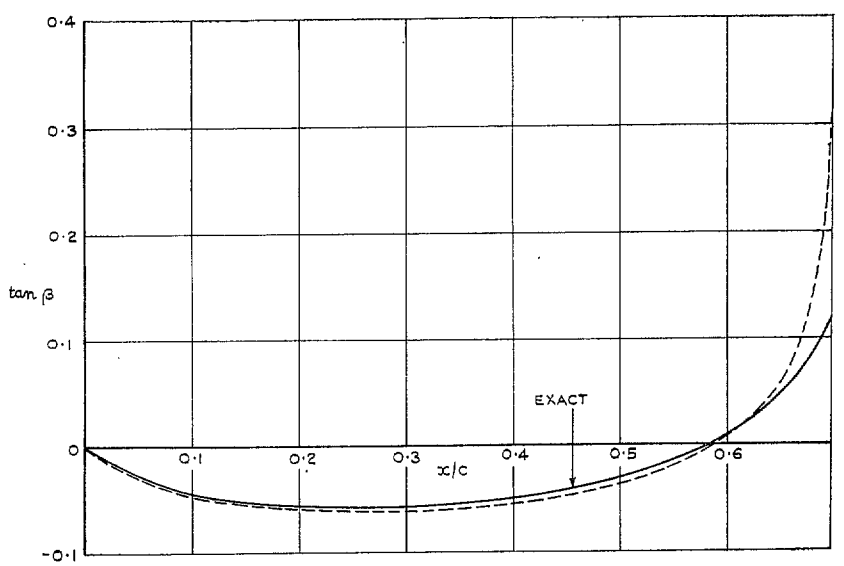

FIG. 10. Values of tan β. Example II.

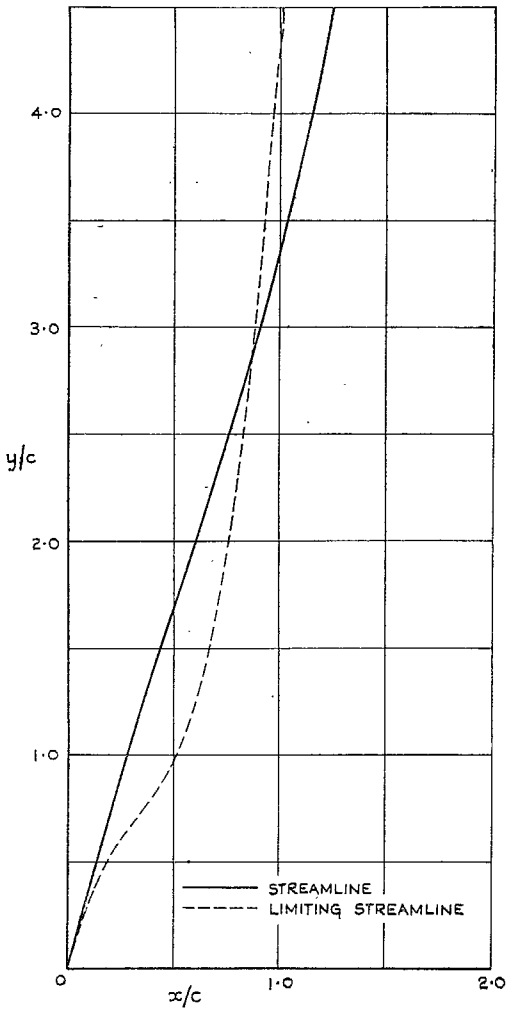

FIG. 11. Streamline and limiting streamline. Example III. Exact.

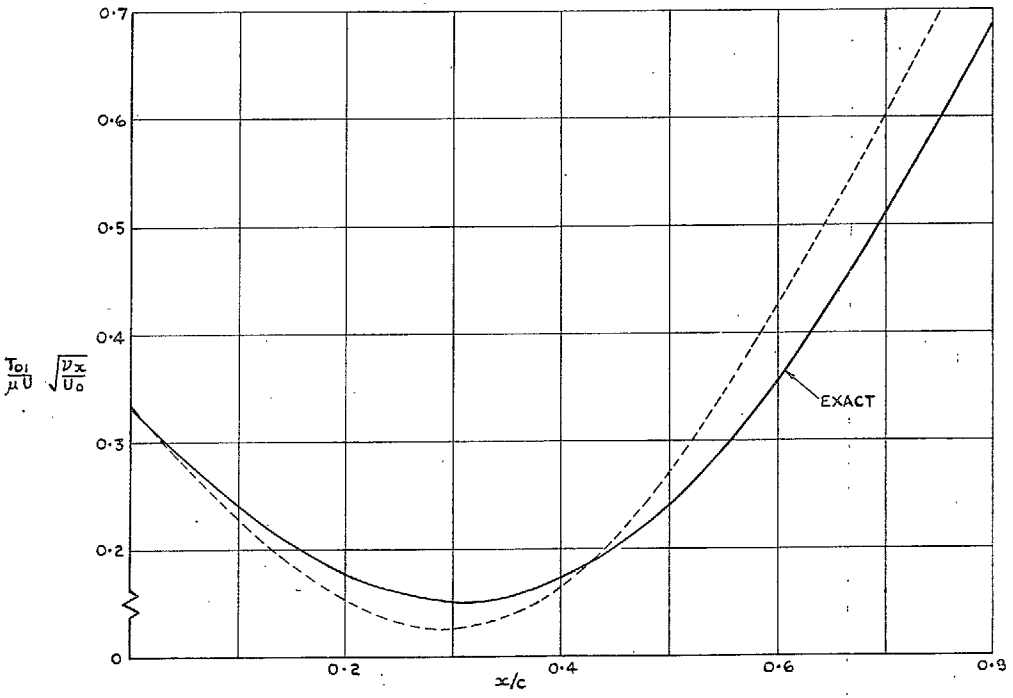

FIG. 12. Streamwise skin friction. Example III.

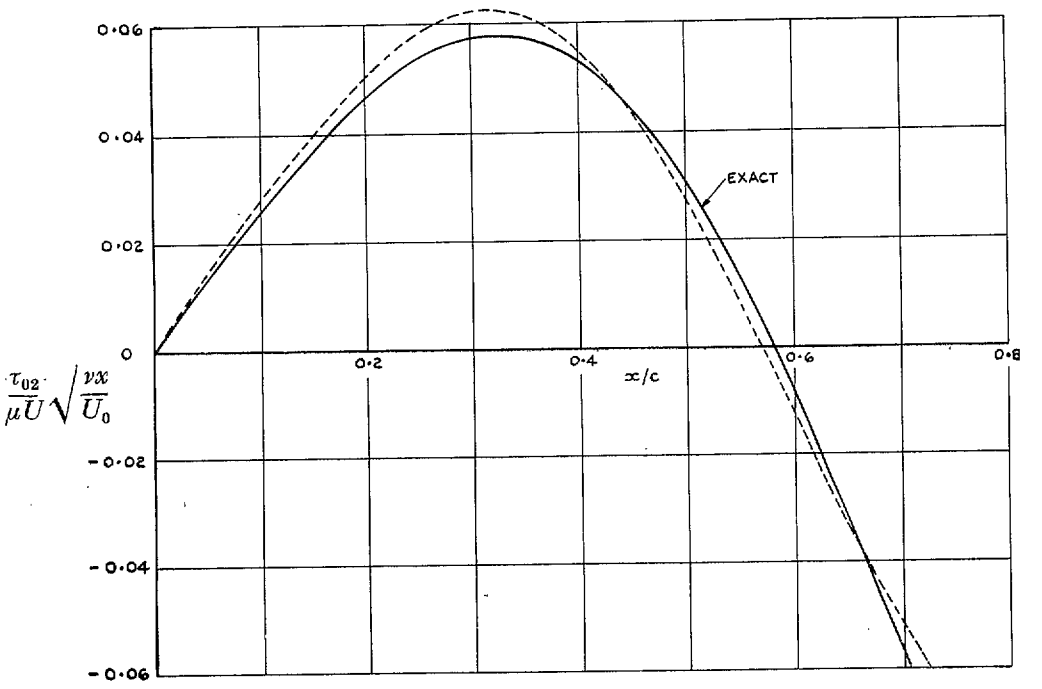

FIG. 13. Cross-flow skin friction. Example III.

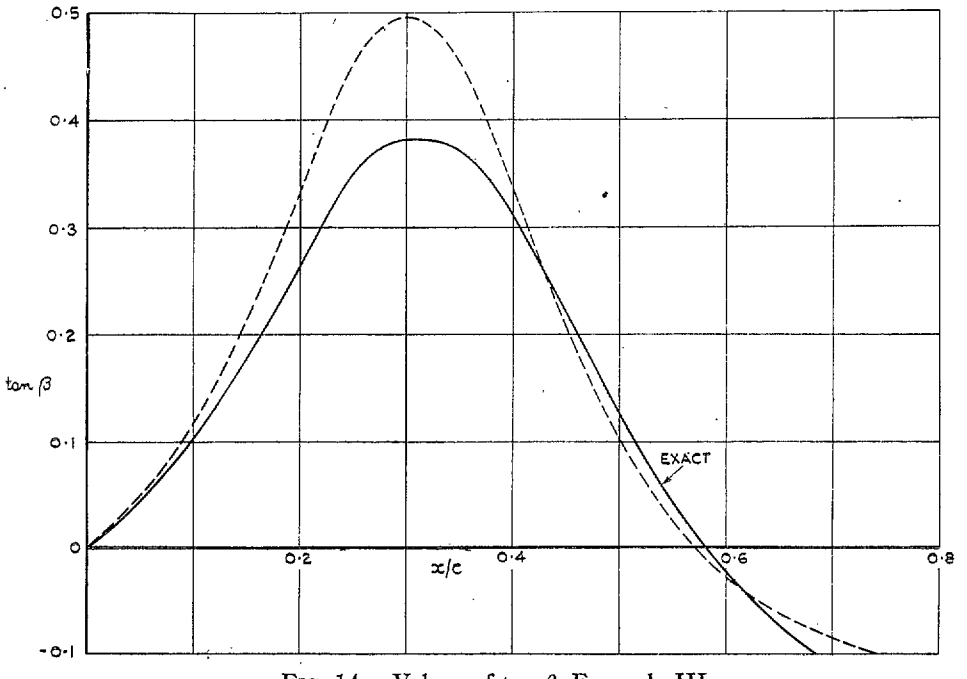

FIG. 14. Values of tan β. Example III.

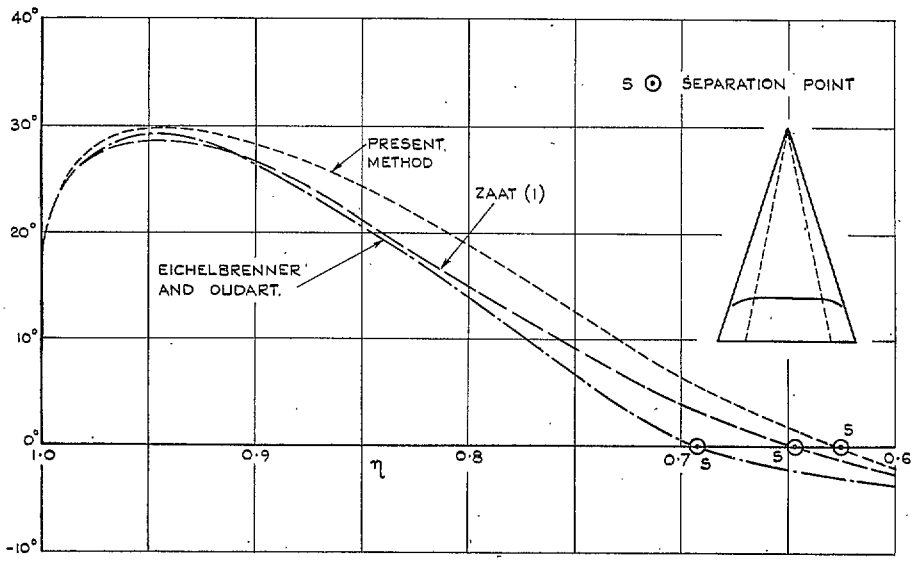

FIG. 15. Angle between limiting streamlines and rays for conically cambered delta wing of Ref. 10 with $n = 2$, $\bar{\eta} = 0{\cdot}6$, $C_L = 0{\cdot}1$, sweepback = 72 deg.

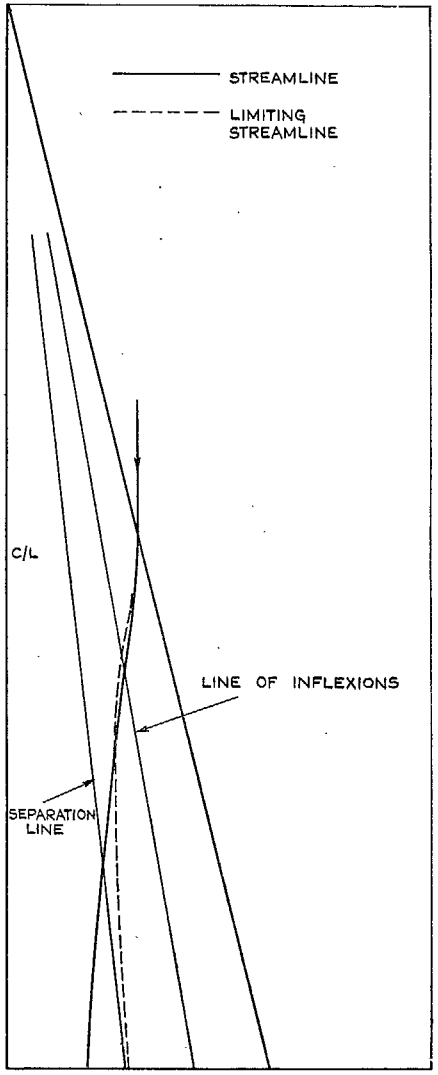

FIG. 16a. Streamline and limiting streamline for conically cambered delta wing of Ref. 10 with $n = 2$, $\bar{\eta} = 0$, $C_L = 0{\cdot}1$. Upper surface.

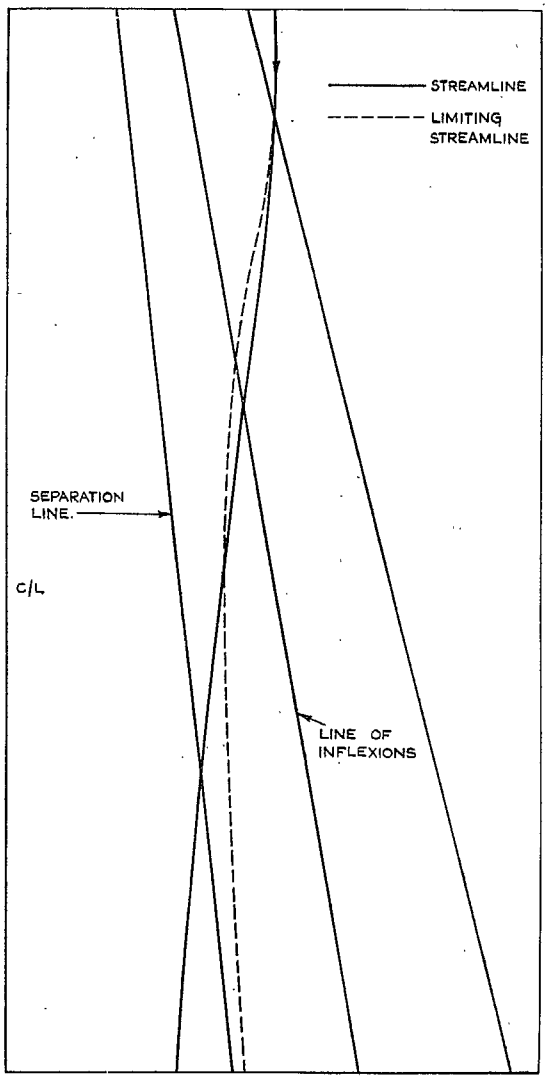

FIG. 16b. Part of FIG. 16a magnified.

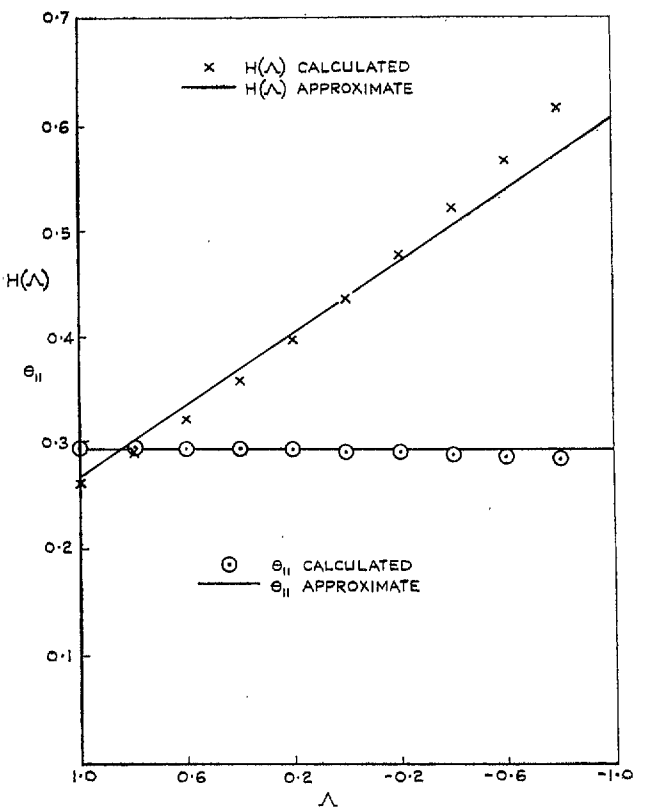

FIG. 17. $H(\Lambda)$ and θ_{11} as functions of Λ.

(50621) Wt. 61 K7 9/60 F. M. & S

Published by
HER MAJESTY'S STATIONERY OFFICE

To be purchased from
York House, Kingsway, London w.c.2
423 Oxford Street, London w.1
13A Castle Street, Edinburgh 2
109 St. Mary Street, Cardiff
39 King Street, Manchester 2
50 Fairfax Street, Bristol 1
2 Edmund Street, Birmingham 3
80 Chichester Street, Belfast 1
or through any bookseller

S.O. Code No. 23-3201